

## Data acquisition considerations for Terrestrial Laser Scanning of forest plots



Phil Wilkes<sup>\*,a,b</sup>, Alvaro Lau<sup>c</sup>, Mathias Disney<sup>a,b</sup>, Kim Calders<sup>a,d</sup>, Andrew Burt<sup>a</sup>, Jose Gonzalez de Tanago<sup>c</sup>, Harm Bartholomeus<sup>c</sup>, Benjamin Brede<sup>c</sup>, Martin Herold<sup>c</sup>

<sup>a</sup>Department of Geography, University College London, Gower Street, London WC1E 6BT, UK

<sup>b</sup>NERC National Center for Earth Observation, UK

<sup>c</sup>Laboratory of Geo-Information Science and Remote Sensing, Wageningen University, P.O. Box 47, Wageningen 6700 AA, the Netherlands

<sup>d</sup>Earth Observation, Climate and Optical Group, National Physical Laboratory, Hampton Road, Teddington, TW11 0LW, UK

### ARTICLE INFO

#### Article history:

Received 6 September 2016

Received in revised form 24 April 2017

Accepted 28 April 2017

Available online 11 May 2017

#### Keywords:

Terrestrial Laser Scanning

Forests

Data acquisition protocol

Above Ground Biomass

Tree structure

### ABSTRACT

The poor constraint of forest Above Ground Biomass (AGB) is responsible, in part, for large uncertainties in modelling future climate scenarios. Terrestrial Laser Scanning (TLS) can be used to derive unbiased and non-destructive estimates of tree structure and volume and can, therefore, be used to address key uncertainties in forest AGB estimates. Here we review our experience of TLS sampling strategies from 27 campaigns conducted over the past 5 years, across tropical and temperate forest plots, where data was captured with a RIEGL VZ-400 laser scanner. The focus is on strategies to derive *Geometrical Modelling* metrics (e.g. tree volume) over forest plots ( $\geq 1$  ha) which require the accurate co-registration of 10s to 100s of individual point clouds. We recommend a 10 m  $\times$  10 m sampling grid as an approach to produce a point cloud with a uniform point distribution, that can resolve higher order branches (down to a few cm in diameter) towards the top of 30+ m canopies and can be captured in a timely fashion i.e.  $\sim 3$ –6 days per ha. A data acquisition protocol, such as presented here, would facilitate data interoperability and inter-comparison of metrics between instruments/groups, from plot to plot and over time.

© 2017 The Authors. Published by Elsevier Inc. This is an open access article under the CC BY license (<http://creativecommons.org/licenses/by/4.0/>).

### 1. Introduction

Uncertainty when modelling the impacts of future climate scenarios is, in a large part, a result of uncertainty in the contribution of the terrestrial ecosystem (Friedlingstein et al., 2006; Sitch et al., 2008). Forests are the predominant terrestrial source and sink of carbon, varying greatly across time and space, and there has been much effort to constrain estimates of the terrestrial carbon pool (Bombelli et al., 2008). Methods to do so have typically involved detailed *in-situ* measurements at the tree or plot level (Chave et al., 2014). More recently these methods have been augmented with remote sensing, including aircraft and satellite observations, particularly airborne LiDAR (Asner et al., 2010). However, all these methods rely on empirical models to generate estimates of Above-Ground Biomass (AGB) and as a result tend to suffer from non-optimal sampling, including small numbers of harvested trees or biased sample size distributions

e.g. under-sampling large trees which contain disproportionate biomass (Clark and Kellner, 2012; Duncanson et al., 2015).

Over the past fifteen years, Terrestrial Laser Scanning (TLS) has proven to be an increasingly practical option for providing precise, accurate, timely and non-destructive estimates of forest biophysical metrics, including AGB (Lovell et al., 2003; Hopkinson et al., 2004; Thies and Spiecker, 2004; Jupp et al., 2008; Calders et al., 2015b; Newnham et al., 2015). Falling instrument costs, improved range, precision and accuracy of measurements and increased capability of software and computing infrastructure to process large datasets, have facilitated operational acquisition of TLS data at a forest plot scale. Increased uptake presents opportunities for inter-comparison of techniques and metrics, as well as establishing longer-term measurements of forest structure for the calibration and validation of satellite products. To improve data-interoperability between campaigns, it is suggested that a minimum data standard and a data acquisition protocol for capturing TLS data in forests is adopted (Calders et al., 2015a). A minimum data standard is dictated by the metric being acquired, this will in turn inform the sample design and the specifications of the instrument used. A formal approach to data

\* Corresponding author.

E-mail address: [p.wilkes@ucl.ac.uk](mailto:p.wilkes@ucl.ac.uk) (P. Wilkes).

acquisition is already common in other disciplines, such as national forest inventories (Tomppo et al., 2010), forest ecology e.g. the Global Ecosystem Monitoring (GEM) network or remote sensing validation e.g. BigFoot.

As the name suggests, TLS instruments are ground-based laser scanners, which have typically been developed for precision surveying applications. Depending on the make and model, TLS instruments scan a Field of View (FoV) ranging from a fixed sector to a complete hemisphere where the angular resolution is configurable in azimuth and zenith resolution to a minimum sampling step. Instruments use either a pulsed (time-of-flight) or continuous frequency modulated (phase-shift) laser that measure the distance to an intercepting surface (Newnham et al., 2015). This, combined with measurements of the scanning mirror's orientation, allows for the precise location of an intercepting surface to be determined. State of the art instruments can fire many millions of laser pulses per scan which create a highly detailed 3D point cloud representation of the scanning domain. Some instruments also have a waveform recording capability which records the intensity of the backscattered signal as a function of time. This can be used to identify multiple interceptions (or returns) from a single outgoing pulse which can be important to penetrate occluding foreground vegetation in dense forests (Calders et al., 2014; Lovell et al., 2003). There are currently no commercially available scanners that are specifically designed for deployment in forests, however, commercial surveying instruments have been used successfully to measure forest structure in great detail (Newnham et al., 2012). Additionally, there are several prototype experimental TLS instruments that have been developed specifically for forest applications, including the single wavelength Echidna (Strahler et al., 2008) and its successor, the Dual Wavelength Echidna Laser scanner (DWEL) (Douglas et al., 2015), and the Salford Advanced Laser Canopy Analyser (SALCA) instruments (Danson et al., 2014; Gaulton et al., 2010).

Biophysical metrics estimated with TLS can be broadly grouped into two categories: *Gap Probability* and *Geometrical Modelling* metrics (Newnham et al., 2015). *Gap Probability* metrics assume that the canopy comprised small “soft” features that are distributed and oriented randomly throughout the scanning domain e.g. leaves and needles in a forest. Examples of *Gap Probability* metrics include direct estimates of gap probability (Danson et al., 2007) as well as derived metrics including Leaf Area Index (Lovell et al., 2003) and Plant Area Volume Density (Jupp et al., 2008). “Soft” features often result in only a fraction of the outgoing pulse being backscattered, therefore *Gap Probability* metrics are derived from the statistical probability of recording an intercept (as a function of scan angle). As *Gap Probability* metrics are derived from probability functions, scans can be treated as independent samples and, therefore, do not require co-registration. *Gap Probability* metrics are often derived from single scans (Jupp et al., 2008; Lovell et al., 2003) or multiple scans integrated to a single point (Calders et al., 2014; Schaefer et al., 2015).

Conversely, *Geometrical Modelling* metrics are derived assuming hard targets (e.g. tree stems and branches) which can be modelled explicitly. Examples include modelling tree structure (Bayer et al., 2013) and volume e.g. using the Quantitative Structure Models or QSM approach (Raumonen et al., 2013; Hackenberg et al., 2015), which in turn can be used to estimate AGB (Calders et al., 2015b). Tree models can also be used in a radiative transfer modelling framework to simulate forests for modelling terrestrial and spaceborne instruments (Calders et al., 2016). A single scan location can suffer from limited sampling of the forest canopy and occlusion of distant vegetation by objects in the foreground; (Hilker et al., 2010; Lovell et al., 2011); therefore a systematic multi-scan location approach and subsequent co-registration is necessary. Co-registration requires the accurate determination of scans relative position to a local datum, scans can then be roto-transformed into a common local reference coordinate system. Methods to achieve a coarse co-registration have

involved the use of tree stem recognition (Henning and Radtke, 2006; Zhang et al., 2016; Liu et al., 2017) or artificial targets that are common between scans. Currently, combining only a handful of scans (<10 scans) covering tens or hundreds of square meters has been reported e.g. Calders et al. (2015b). However, as discussed below, with careful planning a large number of scans (>100) can be combined to provide detailed structural information across large forest plots over many hectares (Calders et al., 2016)(Fig. 1).

### 1.1. Overview

Here we aim to provide a summary of our experiences acquiring TLS data over forest plots to generate *Geometrical Modelling* metrics. This generally holds more challenges with respect to acquisition of *Gap Probability* metrics due to the requirement for accurate (sub-centimeter) co-registration of multiple scans (10s to 100s). The guidance is aimed at practitioners who are planning their own campaigns and, therefore, contains both theoretical and practical considerations. The following section introduces equipment, logistics and sampling considerations for undertaking a TLS campaign. This is followed by a summary of our TLS campaigns completed over the past 5 years, including analysis that highlights the benefits of selecting an appropriate sampling strategy. Finally, recommendations for future campaigns are discussed in Section 5. It should be noted that experience is drawn from using a high specification time-of-flight RIEGL VZ-400 TLS instrument (RIEGL Laser Measurement Systems GmbH), the conclusions drawn are intended for users of this instrument. However, we suggest that the presented sampling framework and other recommendations could be modified to suit coarser resolution or lower powered instruments.

## 2. Equipment, sample design and logistics

### 2.1. Equipment

#### 2.1.1. Laser scanner

As stated above, the guidance provided is drawn from experience with a RIEGL VZ-400 scanner. However, there are a number of alternative laser scanners on the market and choosing the right scanner is a question of budget as well as theoretical and practical requirements. For example, the maximum distance at which a scanner is capable of recording an interception can range from a few to many hundreds of meters; this is an important consideration dependent on likely vegetation density and canopy height. The ability to record single or multiple returns may also preclude an instrument from consideration, if for example, it is to be utilised in dense vegetation where occlusion could significantly reduce range (Calders et al., 2014; Lovell et al., 2003). Scanners can also be heavy ( $\geq 10$  kg) (Newnham et al., 2012), therefore, if field sites are a long distance from an access point then a lighter scanner may be more practical. Power access and battery life may also be important in remote locations; battery charging can take several hours, and power access can be intermittent, so multiple batteries and chargers may be vital. A comprehensive review of scanner technologies, capabilities and limitations are provided by Newnham et al. (2015) and Liang et al. (2016). Ongoing efforts by the Terrestrial LiDAR Scanning Research Coordination Network will also highlight the strengths of different commercial and research instruments, for example between time-of-flight and phase-shift scanners.

TLS instruments are normally mounted on a surveying tripod (Fig. 2). The scanner should be located securely on firm ground e.g. directly into the soil removing any duff where possible. It may then be necessary to level the scanner to within instrument tolerances. Many scanners have a panoramic (limited zenith) FoV and do not scan the complete hemisphere. To achieve full hemispheric coverage



**Fig. 1.** Point cloud of Wytham Woods generated from a TLS campaign where 176 scan positions were co-registered. Concurrent RGB images were captured with each scan, the images and point cloud were then co-registered and points are attributed with an RGB value. An animated fly-through of this scene can be viewed at <https://www.youtube.com/watch?v=RS6q3HMEJK8>.

it is a requirement to scan in both an upright (i.e. the scanning rotation axis is normal to the ground plane) and tilted position, where the scanner is rotated 90° on a tilt mount so the rotation axis is parallel to the ground. The scanner should be positioned so that, as far as is possible, the area surrounding it is free from vegetation up to the minimum distance an interception can be resolved. This is to avoid the instrument mistakenly recording “no data” for the outgoing pulse which may then be interpreted as a canopy gap. Furthermore, objects

in close proximity will also occlude a disproportionate fraction of the FoV.

#### 2.1.2. Retro-reflective targets

To achieve a coarse co-registration, surveys conducted over a number of scan locations require common targets that can be identified in adjacent scans. A reliable and flexible solution is to use a set of temporary retro-reflective targets that are visible from both (or many) scan locations. Targets can be spherical, cylindrical or flat (Fig. 3), for example, Hilker et al. (2010) used polystyrene spheres. Such targets are typically provided by TLS manufacturers, but can also be made quite cheaply and quickly using off-the-shelf components such as retro-reflective tape (see Fig. 3A and B). Spheres and cylinders should be preferred when the targets need to be visible from very different directions. The minimum size of a target is a function of scanner angular resolution, beam divergence, reflectivity of the target, incidence angle of the laser beam on the target and distance of the scanner from target (Alba et al., 2008). The number of returns recorded for a target reduces significantly with increasing distance from the scanner (Calders et al., 2017).

Targets are normally mounted on poles e.g. fencing stakes, which are firmly driven into the ground to prevent movement (bearing in mind they may be *in-situ* for extended periods due to bad weather or being left overnight). To achieve satisfactory registration a minimum of 4 common targets are required between scans, it is therefore advisable to deploy >4 targets for redundancy purposes and to assess registration accuracy. When placing targets it is important that they are not occluded from both (or many scan locations) in the upright and tilt scan locations, this can be checked by ensuring that the laser aperture is clearly visible from the target location. Targets should be spread out within the instrument FoV between the two (or many) scan locations, including as much variation as possible in the vertical direction. Having targets in a relatively narrow FoV may introduce excessive roll or pitch errors in the subsequent co-registration. For example, if all targets are aligned between the two scanners this could introduce an excessive roll error. If a target position changes between scans e.g. becomes loose or is knocked over, this should be removed and placed out of view of the scanner for any subsequent scans. Care should be taken when moving around *in-situ* targets as (re)moving targets can impact co-registration accuracy and significantly increase post processing time. Coloured flagging



**Fig. 2.** A RIEGL VZ-400 TLS instrument deployed in Harwood Forest.

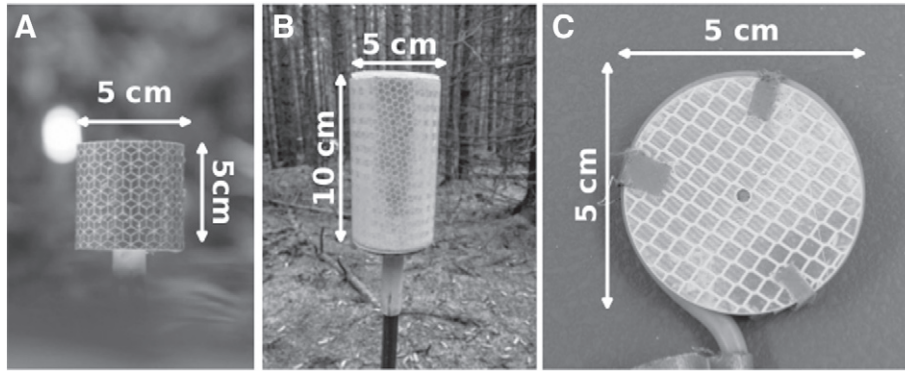


**Fig. 3.** Examples of retro-reflective targets. **A** and **B** are cylindrical, **C** is flat and can either be attached to a surface or mounted on a pole.

tape could be used to identify sets of targets and prevent targets being accidentally moved.

**2.2. Sample design**

There are a number of different configurations and approaches that can be utilised when setting out a sampling grid. The overall aim is to produce a point cloud that (a) captures a large proportion of the target canopy, (b) has a uniform point density across the scanning domain, including vertically (important when applying clustering algorithms e.g. RANSAC (Hackenberg et al., 2015)), and (c) can be co-registered with a desired degree of accuracy. The required co-registration accuracy will depend on the application, but to make best use of the data should be better than the instrument spot size at the closest useful range i.e. of the order of centimeters (for 5–10 m range). Co-registration accuracy can often be improved during post processing with manual refinements e.g. careful selection/pruning of targets and selecting between multiple registration solutions with similar residual errors.

The density of the sampling pattern is determined by the size of the area to be scanned, the density of the vegetation and the metrics to be derived. For example, metrics that require only a coarse resolution scan of the lower portion of the canopy (e.g. stem location) can

be derived from a less dense sampling pattern; whereas, to resolve higher order branches requires a more dense sampling configuration. Discussed below are examples of protocols used for scanning a single tree and area-based scanning of many trees, typically an area  $\geq 1$  ha.

If repeat campaigns are planned (e.g. leaf on and off), then marking the location of each scan position (e.g. with a small flag or stake) is beneficial. When the repeat scan is performed the scanner should ideally be  $< 1$  m from the original location to improve co-registration between scanning acquisitions and to maintain a uniform point density. Another option for repeat scanning is to consider permanently installing a few retro-reflectors in key locations e.g. plot corners, to accurately co-register repeat scans.

**2.2.1. Scanning a single tree**

For scanning a single tree a number of different approaches are available, two of which are discussed below: i) a radial pattern around the tree stem and ii) a regular grid (Fig. 4). Raunonen et al. (2013) suggest a minimum of 3 scan locations to capture a single tree, however, in our experience 6 or more scan locations are required to capture a tree (and surrounding) canopy architecture.

With regard to Fig. 4A, scan locations are located at Cardinal coordinates ( $0^\circ, 30^\circ, 60^\circ, \dots, 300^\circ$ ) around the tree stem. Scanning

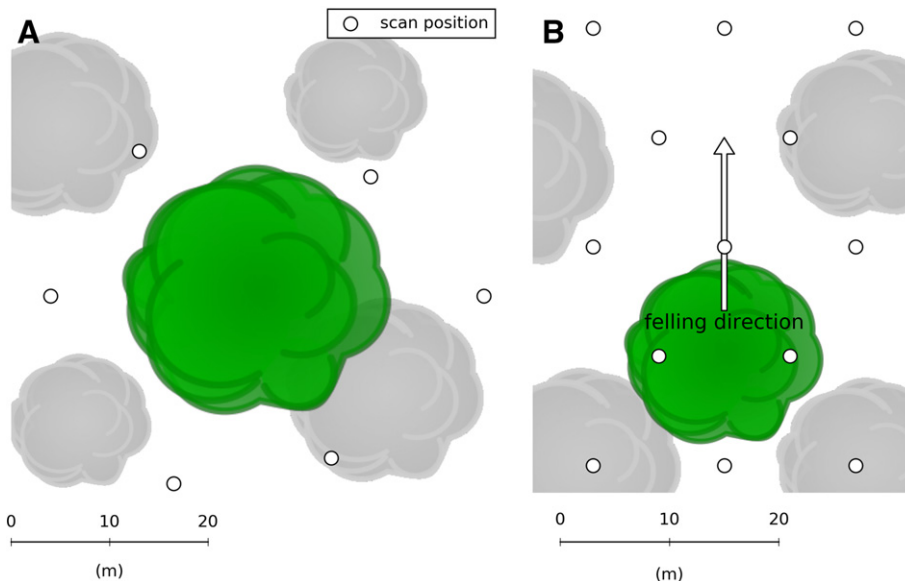


**Fig. 4.** Examples of scan patterns for a single tree where the tree of interest is highlighted in green. **A:** sampling pattern where the scanner is located at  $0^\circ, 60^\circ, \dots, 300^\circ$  around the tree at varying distance from the stem; **B:** a regular grid to sample a tree (and surrounding canopy) pre- and post-harvest.

locations along the axes are subjectively chosen on ability to sight the crown and can be anywhere from 1–40 m from the base of the tree. The example in Fig. 4B is a sampling scheme designed for repeated scans pre- and post-harvest of a large tree, which optimises the sampling of both the harvested and surrounding trees which may be potentially damaged during harvesting. The TLS scan locations followed a systematic grid consisting of a total of 13 scan locations. In each plot, the tree was located at 15 m on the X axis and 5–10 m on the Y axis which was aligned to the expected fall direction of the harvested tree.

Single tree scan configurations have also been extended to capture larger areas e.g. Calders et al. (2015b).

### 2.3. Scanning a large area

When scanning a larger area, a practical, repeatable and scalable approach is to locate scan locations on a systematic grid. Existing grids, established as part of permanent sampling plots (e.g. Rainfor, GEM or Afritron) can be utilised, saving significant time establishing a new plot. Where there are existing plots there is also likely to be existing data e.g. detailed forest inventories, that could prove very useful. When establishing the scanning grid, it is advisable to use the existing plot origin and relative coordinate system to aid co-registration with existing data sets. Co-registration can be further enhanced by identifying (and marking with retro-reflectors) common anchors (e.g. plot corners) that could serve as ground control points.

It is recommended that the overall scan pattern forms a continuous “chain” where each scan location is linked to the previous and next location (Fig. 5A). A number of different configurations have been trialled dependent on stem and understory density. For example, when understory vegetation is dense a higher resolution sampling grid has been used e.g. 10 m × 10 m, to ensure adequate sampling of the canopy through the understory as well as occlusion of adjacent scan locations; whereas, if the understory is more open, a 20 m × 20 m sampling grid has been used. In very dense vegetation, a clear view of the tree canopy may not always be possible; however, it is important to continue a regular scanning “chain” to aid co-registration and maintain a uniform point density.

If the understory is sufficiently open, a sampling configuration as presented in Fig. 5B has been used. Targets are set out on a per row basis where once the end of a row is reached all targets are shifted on to the next row. For the first and last rows, targets are set out in a similar pattern outside of the grid. Targets are also located outside of the plot at the beginning and end of each row. For example, moving left to right in Fig. 5B, targets outside Row 1 and between Row 1 and

2 are used when scanning Row 1. Once Row 1 is complete, the targets outside of Row 1 are moved to between Rows 2 and 3 and Row 2 is scanned. In this example, four targets are used per quadrant, where a quadrant is bounded by a scan location at each corner.

An alternative sampling pattern applicable to more dense vegetation is presented in Fig. 5C. From Scan Location 1 a set of 6 targets are located in view of the scan aperture between Scan Location 1 and Scan Location 2, once scanning is completed the scanner is moved to Scan Location 2. Before scanning at Scan Location 2, a second set of 6 targets is located between Scan Location 2 and 3. After scanning is completed at Scan Location 2, the scanner is moved on to Scan Location 3 and the targets between Scan Locations 1 and 2 are moved to between Scan Locations 3 and 4. Once the end of a row is reached, scanning continues down the next row (Fig. 5A). The rows are linked by placing targets between the first and last scan positions of the adjacent rows as illustrated between Scan Locations 22 and 23 in Fig. 5C.

If tilt scans are required, to ensure that targets are in the instruments FoV it is common practice to align the scanner at each location so that the tilt scan is perpendicular to the direction of the scanning transect i.e. the scanner's rotation axis is perpendicular to the sampling transect. If using the method described in 5C it is important to include an extra target on the outside of the grid at the beginning and end of the scanning chain e.g. Scan Location 1, or at the end of a row (Scan Locations 22 and 23 in Fig. 5C). This is to compensate for the lack of targets outside grid, therefore, reducing roll and pitch errors when co-registering the tilt and upright scans.

### 2.4. Logistics

There are a number of logistical issues to consider when planning a TLS campaign, many of which are common to all remote field work e.g. health and safety considerations. Below is a brief discussion of considerations specific to a TLS campaign.

Forest type, sample design, scanner specifications, instrument settings and weather conditions can all significantly extend the time required to complete a campaign. In good conditions, it is normal for each location to take from 15 min to >1 h to complete, often with the time spent locating targets equalling time the scanner is in operation. There are a number of steps that can be taken to increase time efficiency in the field. For example, it is recommended that scan locations are identified and clearly marked before scanning commences, so that they can be easily located during scanning and used to align subsequent scans and targets. For a large area e.g. 1 ha plot, preparing the plot may take an additional 1–2 days.

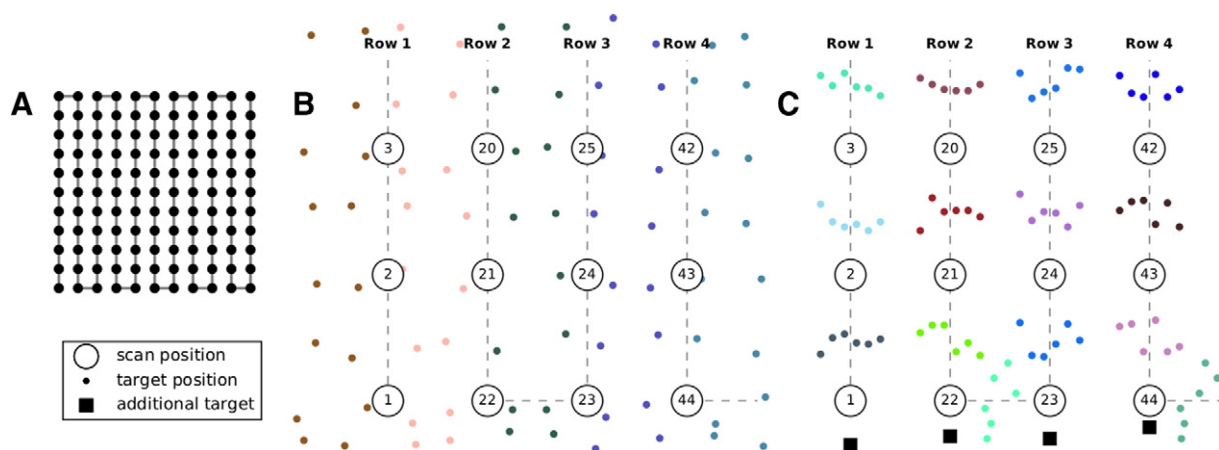


Fig. 5. Sampling pattern configurations for capturing TLS data over large area, where scan locations are linked by a continuous “chain” (A). Examples of sampling patterns where targets are common between rows (B) and between scan locations (C).

**Table 1**  
Field campaigns and specifications. All campaigns used a RIEGL VZ-400 scanner.

Country	Location	Coordinates	Forest type	Stem ha <sup>-1</sup>	
				(10–20 cm dbh)	(≥20 cm dbh)
Australia	Rushworth	36°44'32.30"S 51°145'0.11"E	Eucalypt Open Forest	317–347 <sup>▷</sup>	
Brazil	Caxiuana	1°47'32.30"S 51°26'2.50"W	Lowland tropical rain forest	–	–
Ethopia	Kaffa	7°20'27.68"N 36°13'3.50"E	Forest degradation gradient	289	175
French Guiana	Nouragues	4°4'59.99"S 52°40'59.99"W	Lowland tropical rain forest	–	–
Gabon	Mondah forest reserve	0°34'34.68"N 9°19'23.45"E	Lowland tropical rain forest	460 <sup>▷</sup>	
	Lope National Park <sup>♣</sup>	0°10'29.02"S 11°34'23.98"E	Lowland tropical rain forest	225–393 <sup>▷</sup>	
	Lope (Forest-Savannah Succession)	0°12'12.45"S 11°35'17.38"E	Forest-savannah succession gradient	283–507 <sup>▷</sup>	
Ghana	Ankasa <sup>♣</sup>	5°16'6.75"N 2°41'39.141"W	Lowland tropical rain forest	286	162
	Ankasa (AfriSCAT)	5°16'6.75"N 2°41'39.141"W	Lowland tropical rain forest	~288	~178
	3 single trees <sup>♣</sup>	5°16'6.75"N 2°41'39.141"W	Lowland tropical rain forest	286	162
	Bobiri <sup>♣</sup>	6°41'27.61"N 1°20'18.13"W	Transition forest-savannah and savannah	527–803 <sup>▷</sup>	
	Kogyae <sup>♣</sup>	7°18'9.34"N 1°10'48.65"W	Savannah	193 <sup>▷</sup>	
Guyana	Vaitarna	6°2'13.2"N 58°41'47.4"W	Transition forest-savannah	193–234 <sup>▷</sup>	
		58°41'47.4"W 2°24'43.2"S 113°7'39"E	Lowland tropical rain forest	263	241
Indonesia	Sampit	2°24'43.2"S 113°7'39"E	Peat swamp forest	969	303
Netherlands	Speulderbos	52°15'1.16"N 5°41'56.72"E	Mature Beech forest	11.4	249
Peru	Esperanza <sup>▽</sup>	13°10'32.70"S 71°35'42.05"W	Cloud forest	–	–
	San Pedro <sup>▽</sup>	13°2'56.98"S 71°32'11.40"W	Montane tropical rain-forest	–	–
	Tambopata 05 <sup>▽</sup>	12°49'48.84"S 69°16'13.81"W	Lowland tropical rain forest	–	–
	Tambopata 06 <sup>▽</sup>	12°50'18.438"S 69°17'45.81"W	Lowland tropical rain forest	–	–
	Wayquecha <sup>▽</sup>	13°11'26.63"S 71°35'14.66"W	Cloud forest	–	–
	Madre de Dios	12°16'12"S 69°6'9"W	Lowland tropical rain forest	394	171
	Iquitos	3°50'5.74"S 73°18'53.49"W	Peat swamp forest	546	154
UK	Harwood Forest	50°25'1.00"N 3°50'59.11"W	Conifer plantation	–	–
	Wytham Woods	51°46'31.44"N 1°18'28.08"W	Broadleaf deciduous	232	268

<sup>♣</sup> For A and B refer to Fig. 5B and %C respectively; for C and D refer to Fig. 4A and B respectively

<sup>◇</sup> Tilt scans at higher resolution.

<sup>♠</sup> Global Ecosystem Monitoring network plot <http://gem.tropicalforests.ox.ac.uk/>

<sup>▽</sup> Amazon to Andes transect <http://gem.tropicalforests.ox.ac.uk/projects/aberg>

<sup>▽</sup> Assuming a 3 man team and not including time for travel and poor weather.

<sup>▷</sup> All stems with dbh > 10 cm

Scanner settings can significantly increase time and resources required. For example increasing the angular resolution of the scanner exponentially increases scan time. The decision as to whether to capture discrete return or full-waveform data can also impact the time and resources required. Capturing full-waveform data creates significantly larger files than discrete return data, the RIEGL VZ series full waveform scan files are ~6 – 7 times larger than the discrete return equivalent. This will fill the instrument internal hard drive more quickly and may limit the amount of scanning that can be achieved in a day. Furthermore, by virtue of file size these data are then slower to transfer, view and co-register in post processing. It is suggested that if *Geometrical Modelling* metrics are the aim, then capturing discrete return data is sufficient (Calders et al., 2015b; Burt et al., 2013).

Scanner settings also have implications for the hardware required e.g. additional external batteries and/or data storage. It is recommended that additional batteries and data storage are brought into the field so that scanning can continue even if a battery fails or the instrument's on-board storage is filled.

Scanning is weather dependent and adverse weather conditions may postpone scanning and/or alter canopy conditions significantly. For example, scanning in wet conditions (mist, fog or rain) not only affects the transmission of the laser pulse but also the scattering properties of the leaf surface. Carrying an appropriate wet weather covering for the scanner is advisable for protection during rain showers. Scanning can only resume when leaves are dry and conditions below the canopy are clear. Windy conditions are also not

Year	Angular resolution (°)	Sample pattern*	Mean distance between scan locations (m)	Number of scan locations	Area	Days ha <sup>-1</sup>
2012	0.06	C	40	5	2 plot × 0.5 ha	1
2015	0.04	A	20	36	2 plot × 1 ha	4–5
2015	0.04	C	10–20	5 (centre and 4 on perimeter)	6 plots × 0.03 ha & 21 plots × 0.13 ha	15
2015	0.04	A	20	36	1 plot × 1 ha	4–5
2013	0.06	A	20	36	2 plots × 1 ha	–
2016	0.04	B	10	121	2 plots × 1 ha	5
2013	0.06	A	20	36	1 plot × 1 ha	–
2016	0.06	B	10	121	4 plot × 1 ha	5
2013	0.06	A	20	6	10 plots × 0.08 ha	6
2016	0.04	B	10	121	1 plot × 1 ha	8
2016	0.04	B	10	88	1 plot × 0.7 ha	8
2016	0.04 / 0.01 °	C	~10–20	6–10 per tree	3 single trees	–
2016	0.04	B	10	121	2 plots × 1 ha	3–5
2016	0.04	A	20	36	2 plot × 1 ha	2
2016	0.04	A	10	121	1 plot × 1 ha	2
2014	0.06	D	12.5	13	10 plots × 0.12 ha	4.5
2014	0.06	D	12.5	13	10 plots × 0.12 ha	–
2015–16	0.06	D	14	5	5 plots × 0.04 ha	–
2013	0.06 / 0.009 °	A	20	36	1 plot × 1 ha	5.5
2013	0.06 / 0.002 °	A	20	36	1 plot × 1 ha	5
2013	0.06 / 0.007 °	A	20	36	1 plot × 1 ha	5
2013	0.06 / 0.007 °	A	20	36	1 plot × 1 ha	5
2013	0.06 / 0.007 °	A	20	36	1 plot × 1 ha	5.5
2013	0.06	D	30	8	9 plots × 0.15 ha	–
2013	0.06	C	10	5 (centre and 4 on perimeter)	6 plots × 0.03 ha	–
2015	0.04	A	20	6	1 plot × 0.08 ha	–
2016	0.04	B	10	66	1 plot × 0.5 ha	3
2015–16	0.04	A	20	176	1 plot × 6 ha	2–3

ideal, as even relatively large trees can sway in a light breeze which can produce a ghosting effect in the resulting point cloud. Seidel et al. (2012) recommend scanning in wind speeds of  $<5 \text{ m s}^{-1}$ .

When scanning large areas over extended periods (e.g. many hectares) the impact of phenology or climate must be considered. For example, leaf area and angle may change significantly if scanning through spring (Calders et al., 2015c) or autumn. Changes in season, for example the onset of rainy seasons or snow accumulation, may also significantly alter the structure of the canopy. For this reason it is preferable to time campaigns to when forest conditions and climate are relatively invariant.

It is suggested that a minimum of 2–3 people per team are required to carry and operate equipment, set out targets and identify

scan locations. Equipment can be heavy and awkward to carry through dense vegetation. Having more team members helps distribute the weight and reduces team fatigue, particularly if plots are a distance from access points. We have found that proper training (e.g. scanner functionality, effective reflector placement) and assigning a fixed role to team members each day help to reduce time per location and avoid confusion.

### 3. Analysis

#### 3.1. TLS campaigns

A total of 27 TLS campaigns have been conducted over the past 5 years by our groups, capturing a number of different metrics across a

range of forest types. Acquisitions have ranged from scanning single trees for detailed 3D canopy size and shape analysis, to campaigns across large contiguous areas of commercial plantation, deciduous forest and dense tropical forests to estimate tree volume and biomass (Table 1). Over this time a number of different scan and instrument configurations have been trialled. In the following sections we summarise the evolution of scanning methodologies to capture *Geometric Modelling* metrics and present a brief analysis highlighting the advantages (and disadvantages) of different sampling configurations.

### 3.2. Workflow for processing TLS scans

All scans used in this analysis were first co-registered using RIEGL's RiSCAN PRO<sup>®</sup> software package. A coarse co-registration between scans was achieved using retro-reflective targets as tie-points, as discussed above. Translation and rotation errors were then further reduced using a multi-station adjustment (MSA) approach, MSA modifies the orientation and position of each dataset in several iterations to calculate the best overall fit. Once co-registration was completed, a per-scan rotation and transformation matrix was applied to each raw point cloud to register individual scans into a common local coordinate system. Point clouds were then filtered to remove “noisy” data, these are defined as backscattered pulses that have a significantly different pulse shape when compared to the outgoing pulse (Pfennigbauer and Ullrich, 2010). Differences in pulse shape are often caused by partial backscatter, for example, from leaves or the edge of a stem (Vaccari et al., 2013). Further processing and analysis e.g. tree extraction, was conducted using the *treeseq* software package (Burt, 2017).

### 3.3. Analysis of different sampling configurations

A number of experiments were conducted to highlight the impact of different sample grid densities, total area sampled and appropriateness of a single-tree or grid based approach. Mean Euclidean nearest neighbour distance was used as a metric to compare point cloud density where Euclidean distance was calculated to a point's 4 closest neighbours. This metric provides a forest type agnostic measure of point distribution as, at the scale computed i.e. <10 cm, it is generally independent of the effects of tree spacing and vegetation clumping.

Plot scale analysis was conducted by sub-dividing point clouds into 10 m × 10 m × 10 m voxels. From this, plot scale point cloud uniformity and total area sampled were assessed for different sampling configurations using the nearest neighbour metric. Further analysis was conducted by extracting individual trees from the point cloud. The impact of sampling density was tested on a single tree extracted from the Ankasa AfriSCAT campaign (Table 1) by comparing nearest neighbour distances for data collected on a 10 m grid with data re-sampled to a 20 m and 30 m grid spacing. Distance to scan position was analysed using two trees extracted from the Ankasa GEM plot, a plantation conifer for the 2016 Harwood capture and a tree from the Wytham Woods leaf-on acquisition (Table 1), where each point was classified by Cartesian distance to scan location. Finally, a comparison of a single-tree scanning configuration (Fig. 4A) and a 10 m × 10 m grid based sample design (Fig. 5B) was performed on a tree from the the Ankasa GEM plot captured using both methods.

## 4. Results and discussion

Quantification of global forest carbon sinks and fluxes has been identified as key for understanding future climate change scenarios; to achieve this requires an estimate of forest Above Ground Biomass (AGB). In recent years, Terrestrial Laser Scanning (TLS) methods have proved to be an accurate, timely and non-destructive measurement

tool to estimate standing AGB (Calders et al., 2015b; Hackenberg et al., 2015). Furthermore, as shown here, sampling with TLS can be upscaled to measure numerous trees over many hectares.

An acquisition protocol would assist with data interoperability, inter-comparison of derived metrics between campaigns and for establishing longer-term measurements for calibration and validation purposes. The aim of this guidance, analysis and discussion is to summarise our experience of TLS acquisition for estimating *Geometrical Modelling* metrics. The exact design of an acquisition will be dependent on the target metric and forest conditions, therefore, the information provided here can be scaled accordingly.

### 4.1. Practical considerations

As is the case for field campaigns in other disciplines, TLS data acquisition is ultimately constrained by time, cost and the measurement requirements (area, number, accuracy). As a guide, scanning a 1 ha plot typically takes a team of 3 people between 3 and 8 days (Table 1), dependent upon topography and understorey conditions. External factors including access and weather conditions can significantly increase time required. Often, a large portion of time is spent with the scanner operating; therefore, optimising instrument parameters to given project requirements can maximise cost-benefit. The majority of our campaigns to generate *Geometrical Modelling* metrics have used an angular resolution of 0.04° (Table 1) which has generally satisfied the trade-off between accuracy and time requirements. Increasing scan angular resolution exponentially increases scan length which will reduce number of scan positions possible. The trade-off between capturing high resolution data and capturing data from multiple viewing angles, which can mitigate occlusion particularly towards the top of the canopy, should be considered. If high resolution data are required, restricting the instruments FoV to focus on the target tree can be considered.

Siting retro-reflective targets can also be time consuming. A number of methods have been proposed for a target-less coarse registration, such as the use of tree centres as targets (Henning and Radtke, 2006; Liu et al., 2017) which can then be further augmented by back-sighting the scanner (Zhang et al., 2016). However, target-less approaches are often labour intensive during post-processing (e.g. identifying common targets in adjacent scans) and are only practical when aligning a few scans. Furthermore, in tropical forest it is often the case that the previous scan location is not visible from the next and, therefore, easily identifiable intermediate targets are necessary.

Collaboration can significantly reduce time spent in the field. For example, two laser scanners were used to collect data during the Ankasa campaigns (Table 1); where each team began on opposite ends of the scanning “chain” (Fig. 5A) and eventually met in the middle. As the same specification instrument, scanner settings and sampling method were used by both teams, there were no issues with data interoperability (Calders et al., 2017). Co-registration and post processing were completed as if data were collected from a single instrument so as to avoid compounded co-registration error, particularly towards the point where the two teams met.

### 4.2. Comparison of different sampling strategies

#### 4.2.1. Sampling pattern

When collecting TLS data for the purposes of deriving *Geometric Modelling* metrics, the aim is to produce a point cloud that enables precise co-registration of adjacent scans, has a uniform point distribution and that maximises coverage of the canopy. For all campaigns presented in Table 1, co-registration between scan locations was successful. Using a similar technique, Burt et al. (2013) produced co-registered point clouds with overall registration errors of <1 cm.

The more dense the sampling pattern the more uniform the point distribution (Fig. 6). For example, a higher resolution scan configuration (e.g. 10 m × 10 m) results in a relatively uniform point distribution (Fig. 6A and C). Conversely, a non-uniform distribution of points is produced in the lower portion of the canopy (<10 m) of the Caxiuana and Harwood 2015 plots (Fig. 6B and D) when captured with a 20 m × 20 m sampling pattern. This results in the mean nearest neighbour distance varying by a factor of 5–6, even in the plot centre. Comparing the two Harwood acquisitions, point density is further increased in the 2016 plot by capturing a larger area. A heterogeneous point density may cause errors when applying clustering algorithms that assume a uniform point distribution (Raumonen et al., 2013; Olofsson et al., 2014); therefore, further subsampling (and subsequent information loss) would be required to achieve this. A variable point density may also hinder the identification of smaller trees, particularly in the “gaps” between scan locations.

Furthermore, with increasing understorey density, the placement and sighting of targets becomes more difficult due to occlusion. Typically, a denser sampling pattern makes placement and sighting of targets easier. With increasing height in the canopy and subsequent reduction in vegetation density, the effect of sample density appears to diminish.

For an individual tree, a more dense scan pattern increases the ability to resolve canopy structure, particularly towards the top of the canopy. Fig. 7 compares data from the Ankasa AfriSCAT plot (Table 1) collected on a 10 m grid with data that have been subsampled to a 20 m and 30 m grid spacing. With regard to identifying the tree stem (i.e. canopy height <10 m), mean nearest neighbour distance is <1.5 cm for all scan configurations (compare panels D in Fig. 8). However, in the mid and upper canopy, point spacing increases significantly when comparing the 10 m grid with the 20 m and 30 m patterns (compare panels A, B and C for the different sampling densities in Fig. 7). Differences between sampling densities are particularly evident at the top of the canopy, where increased sample density increases the fidelity of branching structure. The ability to resolve a branch of a certain diameter is a function of the beam

exit diameter, beam divergence and range; therefore, a mean nearest neighbour distance of ~0.03 m is optimal to resolve branches towards the top of a 30 m canopy.

We have found that a good compromise is met by sampling on a 10 m × 10 m grid, this captures data in sufficient detail whilst also permitting capture of large areas on a reasonable time scale. The method illustrated in Fig. 5C is an evolution of the method presented in Fig. 5B and this is now the more commonly used method, owing to reduce time establishing and relocating targets and the requirement for fewer targets overall. The layout illustrated in Fig. 5B may still be useful if TLS is acquired in conjunction with other data captured where (semi)permanent targets are required e.g. mobile or airborne laser scanning (see Section 4.3).

#### 4.2.2. Sampled area

In the lower canopy (i.e. <10 m) the area where mean nearest neighbour distance  $\leq 0.02$  m is often 1.5–3 times the area of the sample grid. For example, the 2016 Harwood campaign sample grid covered an area of 0.5 ha; yet an area of 2.8 ha had a nearest neighbour distance of  $\leq 0.02$  m. The area covered contracts rapidly towards the centre of the plot with increasing height in the canopy (assuming an homogeneous canopy layer, see Fig. 6). For the Ankasa GEM plot, the area where mean nearest neighbour distance is  $\leq 0.02$  m is a factor of 1.6, 1.2 and 0.01 the scanned area for canopy height of 0–10 m, 10–20 m and 20–30 m respectively (Fig. 6A). Similarly for the 2016 Harwood data, the area where mean nearest neighbour distance is  $\leq 0.02$  m is 2.84 and 0.78 times the plot footprint for canopy height 0–10 m and 10–20 m respectively. To maximise area where point density is sufficiently high, as well as simplifying plot establishment, it is suggested that plots are square in shape.

Scan locations from a relatively large distance can contribute significantly to the point cloud that comprise a tree (Fig. 8), this is particularly true towards the top of the canopy. For example, for the Wytham Woods tree in Fig. 8, 45% of returns above a canopy height of 20 m are from scan locations  $\geq 40$  m from the tree.

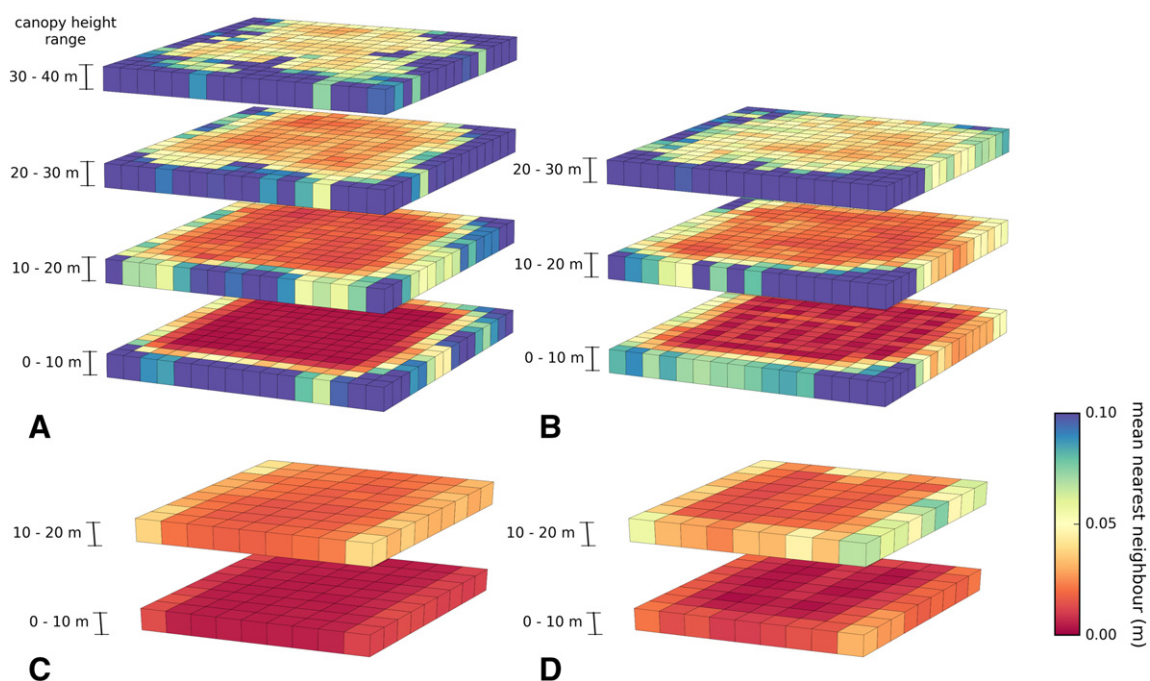


**Fig. 6.** Mean nearest neighbour distance (4 closest neighbours) calculated across forest plots for 10 m × 10 m × 10 m voxels. (A) the Ankasa GEM plot comprising 121 scan locations over 1 ha on a 10 m × 10 m grid, (B) the Caxiuana plot comprising 36 scan locations over 1 ha on a 20 m × 20 m grid, (C) Harwood Forest (2016) comprising 93 scan locations over 0.5 ha on a 10 m × 10 m grid (extent clipped to match plot dimensions of D), and D Harwood Forest (2015) collected over 0.08 ha on a 20 m × 20 m grid over 6 scan locations.

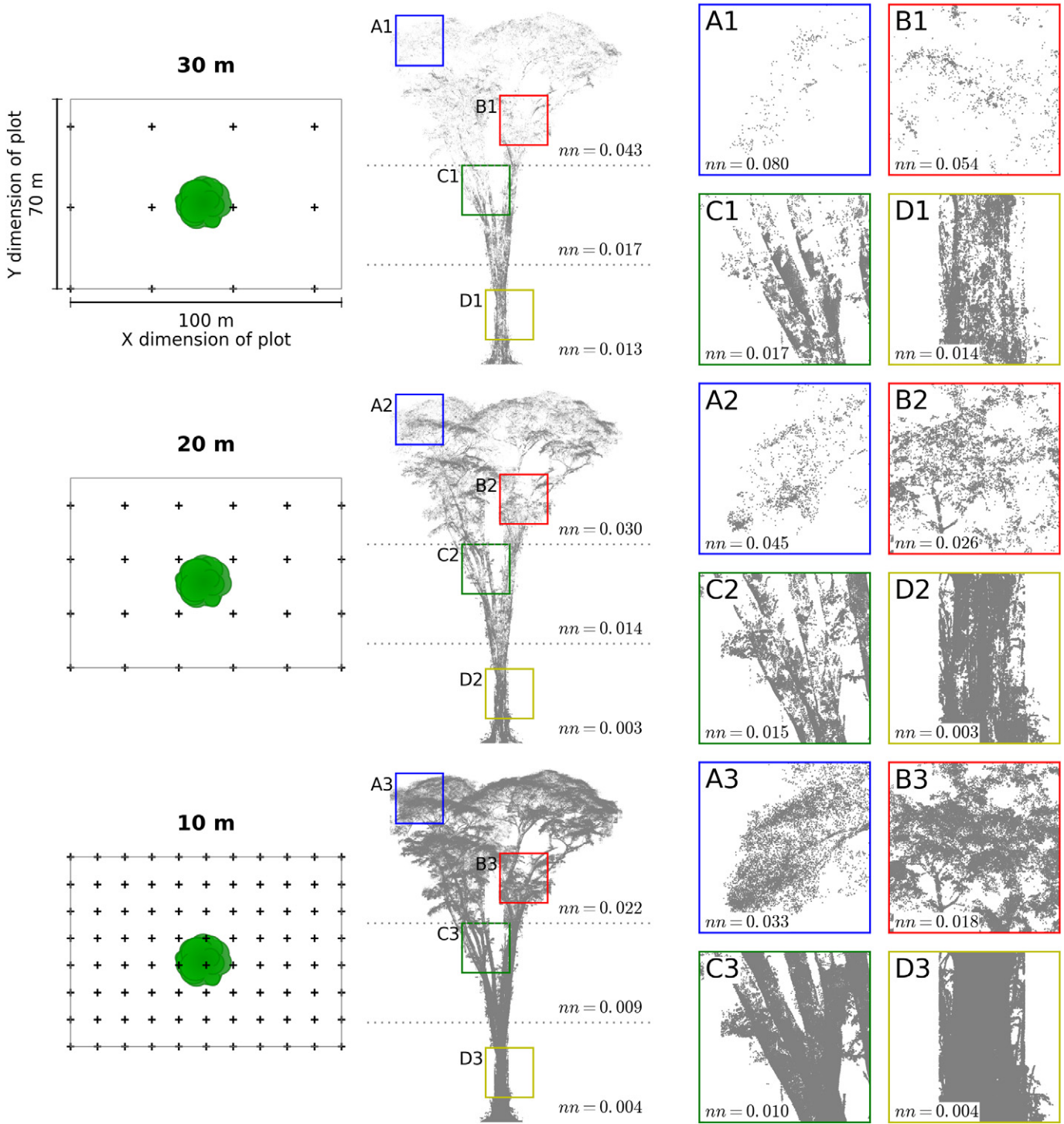


**Fig. 7.** A comparison of mean nearest neighbour distance ( $nn$ ) for points that comprise an individual tree derived using 10, 20 and 30 m grid sampling densities. (left column) The location of sample points and location and extent of the target tree. (middle column) Point cloud representations of the sampled tree including mean nearest neighbour distance for different canopy heights. (right column) Subset  $3\text{ m} \times 3\text{ m} \times 3\text{ m}$  voxels for different areas of the tree, locations are identified in the middle column. The tree has been extracted from the Ankasa AfriSCAT plot (Table 1).

**4.2.3. Single tree vs. grid sampling**

If the primary focus of a campaign is to characterise a single tree, a more focused sample design may be more appropriate than a grid pattern. For example, a scan pattern consisting of 8 scan locations around a target tree, where the tilt scan angular resolution was increased to  $0.01^\circ$ , produced a more vertically consistent cloud when compared to a grid based approach (Fig. 9). However, there

are a couple of points worth noting when comparing the two techniques. Firstly, the contribution of any single scan location maybe limited e.g. due to occlusion, and the contribution of more distant scan locations may not be immediately apparent. As can be in the heat maps of Fig. 8, it is normally one or two scan locations that contribute significantly to a trees' point cloud; however, scan positions  $>50$  away may also contribute significantly. Secondly, the time

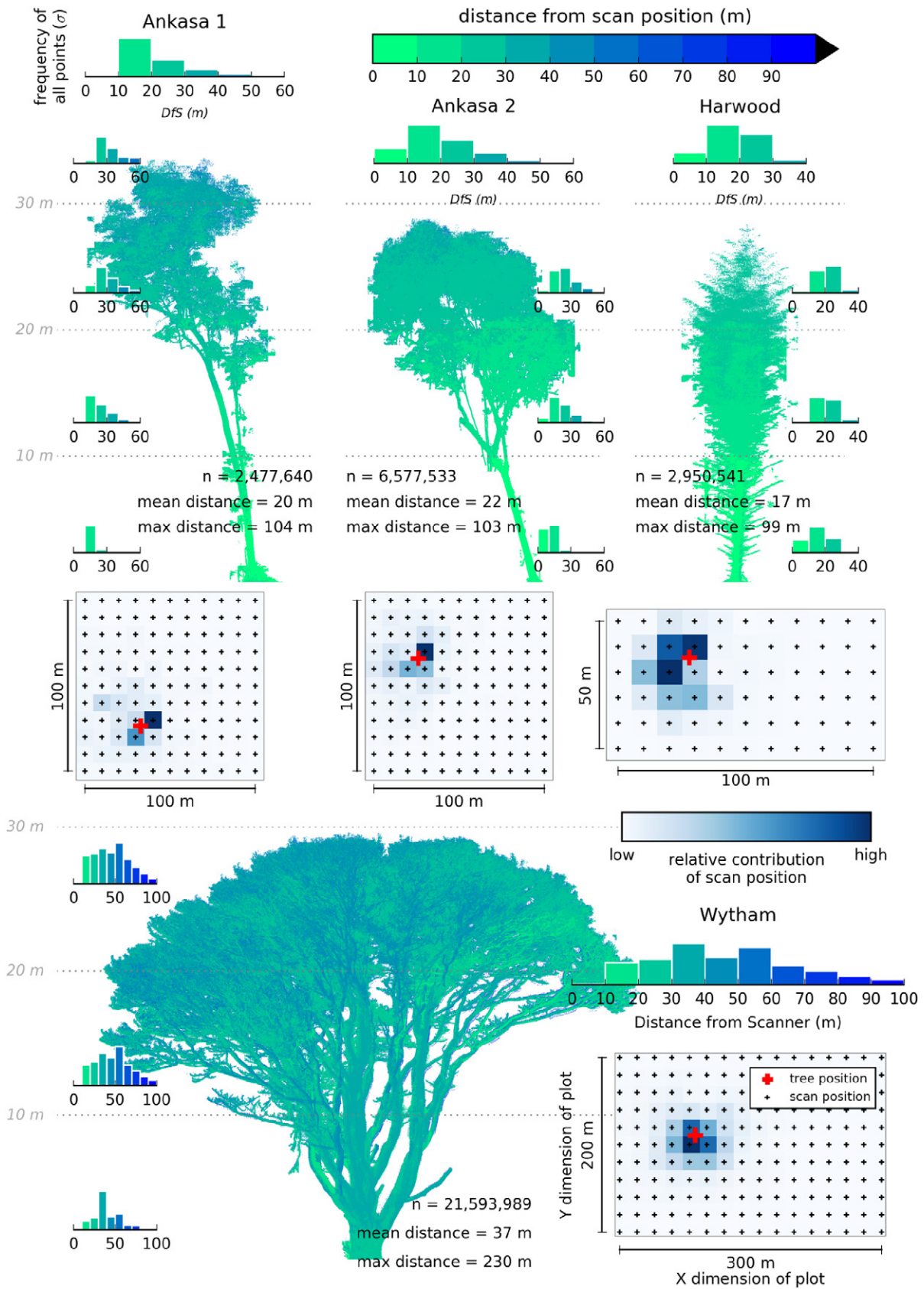


**Fig. 8.** Analysis of distance to scanner for points that comprise four trees; 2 tropical tree from the Anka GEM plot, a Sitka Spruce from Harwood Forest and an Oak tree (leaf-on) from Wytham Woods. Each tree has three panels (top) frequency histograms as a function of scanner distance for all points that comprise a tree, (middle) point cloud representations of the trees, with (inset) frequency histograms for different heights within the canopy and (bottom) heat maps showing the location and relative contribution of the scan positions to each tree. Scanner distances are approximated to the nearest 10m.

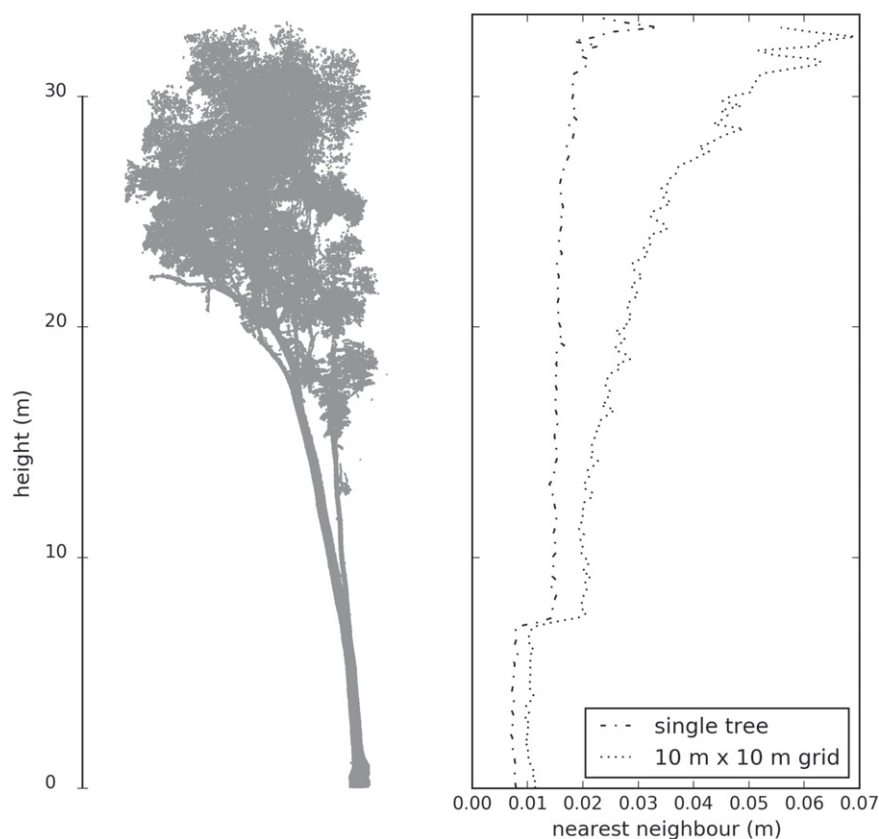


**Fig. 9.** A comparison of mean nearest neighbour distance for a tree captured using a single-tree sampling method (see text) and a 10 m × 10 m grid. The tree was extracted from the Ankasa GEM plot (Table 1).

spent conducting a high resolution single tree scan is far greater than for a grid approach scanning a similar area. For example, the time taken to complete a single scan location for the single tree extraction in Fig. 9 was ~45 min (10 min for an upright scan with a FoV of 360° in azimuth and 100° in zenith at an angular resolution of 0.04° plus 35 min for a tilted scan with a FoV of 100° in both azimuth and zenith at a 0.01° angular resolution); whereas, a single scan location where both the upright and tilt scan have an angular resolution of 0.04° takes ~20 min. Additionally, small sample size has been a criticism of destructive sampling methods for estimating AGB (Clark and Kellner, 2012; Duncanson et al., 2015). We would argue that for most applications a grid based approach provides sufficient detail to characterise tree structure and volume as well as providing a larger sample of trees. The contribution of any single scan position is greater the closer it is sited to the target tree (including canopy); therefore, we recommend that for single-tree approaches scan positions are <10 m from the tree.

A further alternative is a hybrid of the grid and single tree methods. The plot is scanned on a grid as normal, but trees for which higher detail is required are marked in advance with retro-reflective targets e.g. at least 4 flat targets (Fig. 3C) are pinned to the target and surrounding trees. These trees can then be re-scanned using a higher angular resolution, and both sets of data can then be co-registered together.

#### 4.3. Integrating other measurement techniques

There are now a number of different measurement techniques available that could be used in addition or to augment TLS measurements e.g. airborne, UAV and mobile laser scanning, structure-from-motion, digital (hemispherical) photography and canopy analysers

such as the LAI-2200 (Bauwens et al., 2016; Wallace et al., 2016). Coupling different techniques may require alterations to surveying methods, for example, retro-reflective targets may need to be larger, a different shape or laid out on a (semi)permanent grid e.g. Fig. 5B. To aid co-registration, it is advised that data is collected using the same local origin, measurement units and reference coordinate system and that common features are identified during scanning.

## 5. Conclusion

There is an identified requirement for reducing uncertainty in the contribution of forests to the global carbon budget. Techniques that utilise Terrestrial Laser Scanning (TLS) have proven a robust approach for accurately estimating Above Ground Biomass and other forest structure metrics. However, to ensure that estimates are inter-comparable between campaigns and instruments, as well as into the future, there is a need for data to be collected to a minimum standard and following a standard protocol. This guidance and analysis summarises our experience of acquiring TLS data where the goal was to generate *Geometric Modelling* metrics, and is a culmination of 27 field campaigns over 5 years. The focus are scanning configurations that capture data over larger areas (i.e. beyond the range of a single scan) and/or from multiple viewing angles, where scans need to be co-registered.

Sampling method and configuration will always be constrained by available time and resources and this may result in a compromise of data quality (i.e. data resolution). Ideally, point cloud data should have a uniform distribution of points, be of adequate detail to derive the desired metric and allow accurate co-registration of scan locations. We suggest that the most flexible and scalable approach for achieving this is to arrange scan locations on a regular grid, where

adjacent scan locations are linked in a “chain” using common tie-points. Portable retro-reflective targets were found to be a necessary and reliable method for creating tie-points between scans. Following analysis of different scanning patterns and densities, we suggest that a 10 m × 10 m sampling grid is able to provide a uniform point density required for resolving higher order branches towards the top of the canopy and be completed in a reasonable time frame. This approach is now our standard method regardless of forest type. Less dense sampling patterns may well still be suited for characterising the distribution of larger canopy features e.g. tree stems. A large ( $\geq 1$  ha) square plot balances the maximum area where point density is the highest with ease of establishing the plot. If high detail for individual trees is required then a single tree scan pattern, with a higher angular resolution scan, produces a much denser point cloud. However, there is a trade off with time and total sample size (i.e. number of trees scanned), which has been the criticism of previous *in-situ* techniques.

The recommendations presented here are based upon using a RIEGL VZ-400 time-of-flight scanner. Lower powered/resolution instruments will provide less detail and surveying strategies (and expectations) may have to be modified accordingly. Conversely and looking to the future, instruments that record returns from a greater distance, that scan with increased angular resolution in a timely fashion and accurately resolve multiple returns (including radiometric information), will provide a richer data set than is currently possible. Therefore, scanning patterns may be modified to capture a larger area without loss of information. We would argue that despite this, increasing the number of scan locations will always improve results owing to reduced occlusion. Regardless of scanner specifications, the decisions as to which kind of sampling approach to use should be taken carefully, with the application requirements and data interoperability at the forefront of the planning process.

## Acknowledgements

PW is funded by the NERC National Centre for Earth Observation. PW, MD and AB were supported in part by the NERC National Centre for Earth Observation for equipment and travel, via the NERC GREENHOUSE (award NE/K002554/1) for work in Harwood. PW, AL, MD and AB were funded by the European Space Agency through the BIOMASS mission preparatory campaign for work in Ghana. KC was funded through the Metrology for Earth Observation and Climate project (MetEOC-2), grant number ENV55 within the European Metrology Research Programme (EMRP). The EMRP is jointly funded by the EMRP participating countries within EURAMET and the European Union. AB was funded by NERC award NE/N00373X/1 for the Gabon 2016 field work. AL, MH, JGTM, and HB were funded by the US-SilvCarbon research project (14-IG-11132762-350) and by the Norwegian Agency for Development Cooperation (NORAD) and Germany's International Climate Initiative (IKI) through CIFORS Global Comparative Study on REDD+, and the CGIAR Research Program on Forests, Trees and Agroforestry (CRP-FTA) with financial support from the CGIAR Fund. BB was supported by the IDEAS+ project funded by ESA-ESRIN.

The authors would also like to thank the field crews, in particular: Justice Mensah, Cornelius Valk, Alexander Shenkin, Walter Huaraca Huasco, Niall Origo, Matheus Boni Vicari and Darcy Glenn.

## Appendix A. Supplementary data

Supplementary data to this article can be found online at <http://dx.doi.org/10.1016/j.rse.2017.04.030>.

## References

Alba, M., Roncoroni, F., Scaioni, M., 2008. Investigation about the accuracy of target measurement for deformation monitoring. *Int. Arch. Photogramm. Remote. Sens. Spat. Inf. Sci.* 1053–1060.

- Asner, G.P., Powell, G.V., Mascaro, J., Knapp, D.E., Clark, J.K., Jacobson, J., Kennedy-Bowdoin, T., Balaji, A., Paez-Acosta, G., Victoria, E., Secada, L., Valqui, M., Hughes, R.F., 2010. High-resolution forest carbon stocks and emissions in the Amazon. *Proc. Natl. Acad. Sci. U. S. A.* 107, 16738–16742.
- Bauwens, S., Bartholomeus, H., Calders, K., Lejeune, P., 2016. Forest inventory with Terrestrial LiDAR: a comparison of static and hand-held mobile laser scanning. *Forests* 7, 127.
- Bayer, D., Seifert, S., Pretzsch, H., 2013. Structural crown properties of Norway spruce (*Picea abies* [L.] Karst.) and European beech (*Fagus sylvatica* [L.] in mixed versus pure stands revealed by terrestrial laser scanning. *Trees* 27, 1035–1047.
- ECV, Bombelli, A., Avitabile, V., Balzter, H., Marchesini, L.B., Bernoux, M., Brady, M., Hall, R., Hanse, M., Henry, M., Herold, M., Janetos, A., Law, B.E., Manlay, R., Marklund, L.G., Olsson, H., Pandey, D., Saket, M., Schmillius, C., Sessa, R., Edemir, Y., Valentini, R., Wulder, M., 2008. Assessment of the status of the development of the standards for the terrestrial essential climate variables: biomass. Technical Report Global Terrestrial Observing System Rome.
- Burt, A., 2017. New 3D Measurements of Forest Structure. (Ph.D. thesis). University College London.
- Burt, A., Disney, M.I., Raunonen, P., Armston, J.D., Calders, K., Lewis, P., 2013. Rapid characterisation of forest structure from TLS and 3D modelling. *IGARSS*. pp. 3387–3390. Melbourne, Australia, 21st–26th July.
- Calders, K., Armston, J., Newnham, G., Herold, M., Goodwin, N., 2014. Implications of sensor configuration and topography on vertical plant profiles derived from terrestrial LiDAR. *Agric. For. Meteorol.* 194, 104–117.
- Calders, K., Burt, A., Origo, N., Disney, M., Nightingale, J., Raunonen, P., Lewis, P.E., 2016. Large-area virtual forests from terrestrial laser scanning data. *IEEE International Geoscience and Remote Sensing Symposium 2016 10–15 July 2016* (pp. 1765–1767). Beijing, China.
- Calders, K., Disney, M.I., Armston, J.D., Burt, A., Brede, B., Origo, N., Muir, J., Nightingale, J., 2017. Evaluation of the range accuracy and the radiometric calibration of multiple terrestrial laser scanning instruments for data interoperability. *IEEE Trans. Geosci. Remote Sens.* 1–9.
- Calders, K., Newnham, G.J., Armston, J.D., Disney, M.I., Schaaf, C.B., Paynter, I., 2015a. Terrestrial LiDAR for forest monitoring. A sourcebook of methods and procedures for monitoring and reporting anthropogenic greenhouse gas emissions and removals associated with deforestation, gains and losses of carbon stocks in forests remaining forests, and forestation. *GOCF-GOLD Land Cover Project Office, Wageningen University, The Netherlands*. (Gocf-gold ed.).
- Calders, K., Newnham, G.J., Burt, A., Murphy, S., Raunonen, P., Herold, M., Culvenor, A., Avitabile, V., Disney, M.I., Armston, J.D., Kaasalainen, M., 2015b. Nondestructive estimates of above-ground biomass using terrestrial laser scanning. *Methods Ecol. Evol.* 6, 198–208.
- Calders, K., Schenkels, T., Bartholomeus, H., Armston, J.D., Verbesselt, J., Herold, M., 2015c. Monitoring spring phenology with high temporal resolution terrestrial LiDAR measurements. *Agric. For. Meteorol.* 203, 158–168.
- Chave, J., Réjou-Méchain, M., Búrquez, A., Chidumayo, E., Colgan, M.S., Delitti, W.B.C., Duque, A., Eid, T., Fearnside, P.M., Goodman, R.C., Henry, M., Martínez-Yrizar, A., Mugasha, W. a., Muller-Landau, H.C., Mencuccini, M., Nelson, B.W., Ngomanda, A., Nogueira, E.M., Ortiz-Malavassi, E., Pélissier, R., Ploton, P., Ryan, C.M., Saldaña, J.G., Vieilledent, G., 2014. Improved allometric models to estimate the aboveground biomass of tropical trees. *Glob. Chang. Biol.* 20, 3177–3190.
- Clark, D.B., Kellner, J.R., 2012. Tropical forest biomass estimation and the fallacy of misplaced concreteness. *J. Veg. Sci.* 23, 1191–1196.
- Danson, F.M., Gaulton, R., Armitage, R.P., Disney, M.I., Gunawan, O., Lewis, P.E., Pearson, G., Ramirez, A.F., 2014. Developing a dual-wavelength full-waveform terrestrial laser scanner to characterize forest canopy structure. *Agric. For. Meteorol.* 198–199, 7–14.
- Danson, F.M., Hetherington, D., Morsdorf, F., Koetz, B., Allgöwer, B., 2007. Forest canopy gap fraction from terrestrial laser scanning. *IEEE Geosci. Remote Sens. Lett.* 4, 157–160.
- Douglas, E.S., Martel, J., Li, Z., Howe, G., Hewawasam, K., Marshall, R.A., Schaaf, C.B., Cook, T.A., Newnham, G.J., Strahler, A.H., Chakrabarti, S., 2015. Finding leaves in the forest: the dual-wavelength Echidna lidar. *IEEE Geosci. Remote Sens. Lett.* 12, 776–780.
- Duncanson, L., Rourke, O., Dubayah, R.O., 2015. Small sample sizes yield biased allometric equations in temperate forests. *Sci. Report.* 5, 17153.
- Friedlingstein, P., Cox, P., Betts, R., Bopp, L., von Bloh, W., Brovkin, V., Cadule, P., Doney, S., Eby, M., Fung, I., Bala, G., John, J., Jones, C., Joos, F., Kato, T., Kawamiya, M., Knorr, W., Lindsay, K., Matthews, H., Raddatz, T., Rayner, P., Reick, C., Roeckner, E., Schnitzler, K.-G., Schnur, R., Strassmann, K., Weaver, A., Yoshikawa, C., Zeng, N., 2006. Climate carbon cycle feedback analysis: results from the C4 MIP model intercomparison. *J. Clim.* 19, 3337–3353.
- Gaulton, R., Danson, F.M., Pearson, G., Lewis, P.E., Disney, M., 2010. The Salford Advanced Laser Canopy Analyser (SALCA): a multispectral full waveform LiDAR for improved vegetation characterisation. *The Remote Sensing and Photogrammetry Society Conference: Remote Sensing and the Carbon Cycle*, London.
- Hackenberg, J., Spiecker, H., Calders, K., Disney, M.I., Raunonen, P., 2015. SimpleTree an efficient open source tool to build tree models from TLS clouds. *Forests* 6, 4245–4294.
- Henning, J., Radtke, P.J., 2006. Detailed stem measurements of standing trees from ground-based scanning lidar. *Forensic Sci.* 52, 67.
- Hilker, T., Leeuwen, M., Coops, N.C., Wulder, M.A., Newnham, G.J., Jupp, D.L., Culvenor, D.S., 2010. Comparing canopy metrics derived from terrestrial and airborne laser scanning in a Douglas-fir dominated forest stand. *Trees* 24, 819–832.
- Hopkinson, C., Chasmer, L., Young-Pow, C., Treitz, P., 2004. Assessing forest metrics with a ground-based scanning lidar. *Can. J. For. Res.* 34, 573–583.

- Jupp, D.L., Culvenor, D.S., Lovell, J.L., Newnham, G.J., Strahler, A.H., Woodcock, C.E., 2008. Estimating forest LAI profiles and structural parameters using a ground-based laser called 'Echidna'. *Tree Physiol.* 29, 171–181.
- Liang, X., Kankare, V., Hyypää, J., Wang, Y., Kukko, A., Haggrén, H., Yu, X., Kaartinen, H., Jaakkola, A., Guan, F., Holopainen, M., Vastaranta, M., 2016. Terrestrial laser scanning in forest inventories. *ISPRS J. Photogramm. Remote Sens.* 115, 63–77.
- Liu, J., Liang, X., Hyypää, J., Yu, X., Lehtomäki, M., Pyörälä, J., Zhu, L., Wang, Y., Chen, R., 2017. Automated matching of multiple terrestrial laser scans for stem mapping without the use of artificial references. *Int. J. Appl. Earth Obs. Geoinf.* 56, 13–23.
- Lovell, J.L., Jupp, D., Newnham, G., Culvenor, D., 2011. Measuring tree stem diameters using intensity profiles from ground-based scanning lidar from a fixed viewpoint. *ISPRS J. Photogramm. Remote Sens.* 66, 46–55.
- Lovell, J.L., Jupp, D.L., Culvenor, D.S., Coops, N.C., 2003. Using airborne and ground-based ranging lidar to measure canopy structure in Australian forests. *Can. J. Remote Sens.* 29, 607–622.
- Newnham, G.J., Armston, J.D., Calders, K., Disney, M.I., Lovell, J.L., Schaaf, C.B., Strahler, A.H., Danson, F.M., 2015. Terrestrial laser scanning for plot-scale forest measurement. *Curr. Forestry Rep.* 1, 239–251.
- Newnham, G.J., Armston, J.D., Muir, J., Goodwin, N., Tindall, D., Culvenor, D., Püschel, P., Nyström, M., Johansen, K., 2012. Evaluation of Terrestrial Laser Scanners for Measuring Vegetation Structure. Technical Report Manuscript ID: EP124571.
- Olofsson, K., Holmgren, J., Olsson, H., 2014. Tree stem and height measurements using terrestrial laser scanning and the RANSAC algorithm. *Remote Sens.* 6, 4323–4344.
- Pfennigbauer, M., Ullrich, A., 2010. Improving quality of laser scanning data acquisition through calibrated amplitude and pulse deviation measurement. In: Turner, M.D., Kamerman, G.W. (Eds.), *PIE 7684, Laser Radar Technology and Applications XV*. vol. 7684, pp. 76841F.
- Raunonen, P., Kaasalainen, M., Åkerblom, M., Kaasalainen, S., Kaartinen, H., Vastaranta, M., Holopainen, M., Disney, M.I., Lewis, P.E., 2013. Fast automatic precision tree models from terrestrial laser scanner data. *Remote Sens.* 5, 491–520.
- Schaefer, M.T., Farmer, E., Soto-berelov, M., Woodgate, W., Jones, S.D., 2015. Overview of ground based techniques for estimating LAI. In: Held, A., Phinn, S., Soto-berelov, M., Jones, S.D. (Eds.), *AusCover Good Practice Guidelines: A technical handbook supporting calibration and validation activities of remotely sensed data products*. chapter 6. (Version 2 ed.).
- Seidel, D., Fleck, S., Leuschner, C., 2012. Analyzing forest canopies with ground-based laser scanning: a comparison with hemispherical photography. *Agric. For. Meteorol.* 154–155, 1–8.
- Sitch, S., Huntingford, C., Gedney, N., Levy, P., Lomas, M., Piao, S., Betts, R., Ciais, P., Cox, P., Friedlingstein, P., Jones, C., Prentice, I., Woodward, F., 2008. Evaluation of the terrestrial carbon cycle, future plant geography and climate-carbon cycle feedbacks using five Dynamic Global Vegetation Models (DGVMs). *Glob. Chang. Biol.* 14, 2015–2039.
- Strahler, A.H., Jupp, D.L., Woodcock, C.E., Schaaf, C.B., Yao, T., Zhao, F., Yang, X., Lovell, J.L., Culvenor, D.S., Newnham, G.J., Ni-Meister, W., Boykin-Morris, W., 2008. Retrieval of forest structural parameters using a ground-based lidar instrument (Echidna®). *Can. J. Remote Sens.* 34, S426–S440.
- Thies, M., Spiecker, H., 2004. Evaluation and future prospects of terrestrial laser scanning for standardized forest inventories. *i* 36, 192–197.
- Tomppo, E., Gschwantner, T., Lawrence, M., McRoberts, R.E. (Eds.), 2010. *National forest inventories pathways for common reporting*. Springer, Heidelberg.
- Vaccari, S., van Leeuwen, M., Calders, K., Coops, N.C., Herold, M., 2013. Bias in lidar-based canopy gap fraction estimates. *Remote Sens. Lett.* 4, 391–399.
- Wallace, L., Lucieer, A., Malenovsky, Z., Turner, D., Vopěnka, P., 2016. Assessment of forest structure using two UAV techniques: a comparison of airborne laser scanning and structure from motion (SfM) point clouds. *Forests* 7, 1–16.
- Zhang, W., Chen, Y., Wang, H., Chen, M., Wang, X., Yan, G., 2016. Efficient registration of terrestrial LiDAR scans using a coarse-to-fine strategy for forestry applications. *Agric. For. Meteorol.* 225, 8–23.